

DOI: 10.1002/sml.200500234

Substrate-Friendly Synthesis of Metal Oxide Nanostructures Using a Hotplate**

Ting Yu, Yanwu Zhu, Xiaojing Xu, Kuan-Song Yeong, Zexiang Shen, Ping Chen, Chwee-Teck Lim, John Thiam-Leong Thong, and Chong-Haur Sow*

Nanostructures with large surface areas and possible quantum-confinement effects exhibit distinct electronic, optical, mechanical, and thermal properties and are believed to be essential to much of modern science and technology.^[1] Some of the most important and widely studied candidates in the family of nanomaterials are metal oxide nanostructures. This is due to their great potential in addressing some fundamental scientific issues on low dimensionality and applications thereof. These include chemical or biological sensors, electron-field emitters, electrodes of lithium-ion batteries, lasers, and optical switches for nanoscale memory and logic devices.^[2] Many techniques have been developed to synthesize metal oxide nanostructures, including an ethylene glycol mediated synthesis,^[3] a carbothermal reduction process,^[4] a vapor–liquid–solid (VLS) process,^[5] and a vapor–solid (VS) process.^[6–8] Among these methods, the VS and VLS processes are well suited for the synthesis of metal oxide nanostructures with single-crystalline structures and in relatively large quantities. For example, Ga₂O₃ and ZnO

nanowires have been synthesized by heating powders of these materials to elevated temperatures in a tube furnace;^[6] oxide nanowires of low-melting-point metals, such as Zn, Mg, and Ge, could be fabricated by directly heating metal powders in a tube furnace under appropriate oxygen atmospheres.^[7] Besides wire-shaped nanostructures, semi-conducting metal oxide nanobelts were also successfully created.^[8] Both VS and VLS processes require careful control of the growth conditions. For example, to generate vapor sources, normally elevated formation temperatures are necessary ($\geq 1000^\circ\text{C}$).^[8] The appropriate atmosphere, flow rate, and substrate position must be carefully controlled.^[8] For the VLS process, an appropriate catalyst must be selected, and subsequently the properties of the nanostructures may be modified because of the catalyst introduced.^[1]

As new techniques for the synthesis of nanomaterials are continuously being discovered, it is also important to develop a method with more practical attributes. Some of the desirable, practical attributes of a new synthesis technique include mass production, rapid growth, catalyst-free, diversity of materials made, low-formation temperature, reasonably low costs,^[1] and ease of nanomaterials assembly onto various substrates for further characterization and applications.^[9] Here, we report a novel and yet surprisingly simple method to synthesize metal oxide ($\alpha\text{-Fe}_2\text{O}_3$, Co₃O₄, and ZnO) nanostructures by directly heating metal-foil- or metal-film-coated substrates in air using a hotplate (hereafter called the hotplate method). Successful attempts have been achieved on a wide variety of substrates, such as a plain silicon wafer, a glass slide, quartz, a silica microsphere, atomic force microscopy (AFM) tips, and electrochemically etched W tips.

Our prior attempts with the hotplate technique created CuO nanowires on Cu foil,^[10] ZnO nanostructures on Zn foil,^[11] and Co₃O₄ on Co foil.^[12] In this work, we extend this method to another high-melting-point metal, iron (Fe, melting point: 1538°C),^[13] and synthesize single-crystalline $\alpha\text{-Fe}_2\text{O}_3$ (hematite) nanoflakes by heating Fe foil directly in air. More importantly, we further develop this method to be able to directly synthesize the nanostructures on a wide variety of substrates. In this report, we demonstrate this hotplate method by focusing on $\alpha\text{-Fe}_2\text{O}_3$ nanoflakes. $\alpha\text{-Fe}_2\text{O}_3$ has been extensively used in the production of gas sensors, catalysts, and pigments.^[14] Nanoscale $\alpha\text{-Fe}_2\text{O}_3$ with different morphologies, such as nanoparticles,^[15] nanorods,^[16] and nanotubes,^[14] has been successfully synthesized and exhibits promising applications. However, to the best of our knowledge, there has been no report for the preparation of $\alpha\text{-Fe}_2\text{O}_3$ two-dimensional (2D) nanostructures. As an illustration of how a new morphology may generate new properties for nanostructures, we investigate the field-emission properties of $\alpha\text{-Fe}_2\text{O}_3$ nanoflakes for the first time.

Optical pictures of a piece of iron foil (10 cm \times 10 cm) during the heating process were captured. Figures 1a–c show the foil before heating, after heating at 300°C for 10 min, and after heating at 300°C for 24 h, respectively. The shiny surface of the Fe foils rapidly became dull and gray, and eventually became dark for long heating durations. Figures 1d–f show the corresponding SEM images of the

[*] Dr. T. Yu, Y. Zhu, Dr. P. Chen, Prof. C.-H. Sow
Department of Physics, Blk S12, Faculty of Science
National University of Singapore
2 Science Drive 3, Singapore 117542 (Singapore)
Fax: (+65) 6777-6126
E-mail: physowch@nus.edu.sg

Y. Zhu, Dr. X. Xu, K.-S. Yeong, Prof. C.-T. Lim, Prof. J. T.-L. Thong,
Prof. C.-H. Sow

National University of Singapore Nanoscience and
Nanotechnology Initiative, Blk S13
2 Science Drive 3, Singapore 117542 (Singapore)

Dr. X. Xu, Prof. C.-T. Lim
Department of Mechanical Engineering
National University of Singapore, Blk E3A
9 Engineering Drive 1, Singapore 117576 (Singapore)

Prof. J. T.-L. Thong
Department of Electrical and Computer Engineering
National University of Singapore, Blk E4
4 Engineering Drive 3, Singapore 117576 (Singapore)

Prof. Z. Shen
Division of Physics and Applied Physics
Nanyang Technological University
1 Nanyang Walk, Block 5, Singapore 637616 (Singapore)

[**] The authors acknowledge the support of NUSARF and NUSNNI. T.Y. acknowledges the support of a Fellowship from the Singapore Millennium Foundation.

Supporting information for this article is available on the WWW under <http://www.small-journal.com> or from the author.

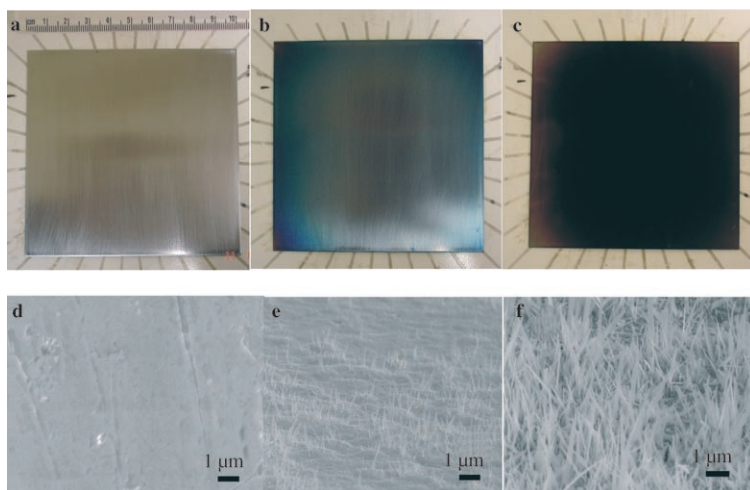


Figure 1. Fabrication of $\alpha\text{-Fe}_2\text{O}_3$ nanoflakes on Fe foil. Optical images of the Fe foil a) before heating, b, c) after heating at $300\text{ }^\circ\text{C}$ for 10 min and 24 h, respectively. d–f) Corresponding scanning electron microscopy (SEM) images of the foil surfaces shown in (a–c). The size of the nanoflakes shows a dramatic increase after heating for a long duration. The growth is rapid and over a large area ($10\text{ cm} \times 10\text{ cm}$).

surface of the foil at the different stages of heating. Figure 1e reveals that the surface is covered with flake-like nanostructures with a typical length of $1\text{ }\mu\text{m}$, root width of 100 nm , and thickness of 10 nm (measured at the middle of the tips).

To illustrate the ease of direct synthesis of these nanostructures onto different substrates, we deposited an Fe film on different types of substrates and heated the coated samples in air. Figure 2a shows an SEM image of nanoflakes synthesized on plain Si, whereas Figure 2b shows the side view of the nanoflake-covered Si. We could also synthesize nanoflakes on a monolayer of silica microspheres (Figure 2c) and individual spheres (Figure 2c, inset). Other substrates include a glass slide (Figure 2d), an AFM cantilever tip (Figure 2e), and an electrochemically etched tungsten tip (Figure 2f). The inset in Figure 2d shows the as-deposited sample (black) becomes transparent (red) after heating. It is interesting to note that most of the

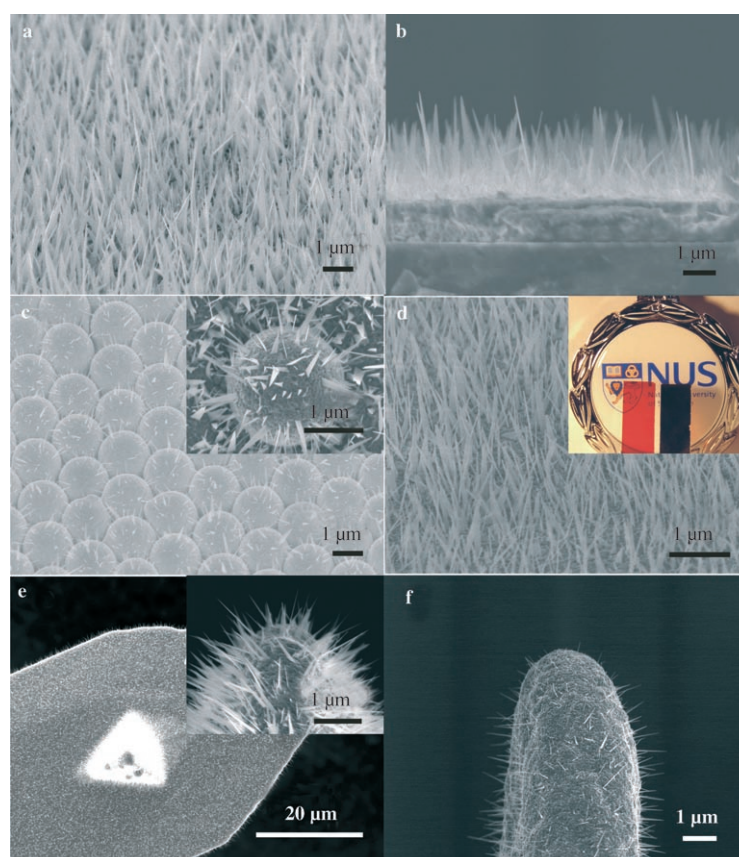


Figure 2. SEM images of $\alpha\text{-Fe}_2\text{O}_3$ nanoflakes synthesized directly on different substrates. a) Nanoflakes synthesized on plain Si and b) a side view of the nanoflake-covered Si. c) Nanoflakes synthesized on a monolayer of silica microspheres. The inset shows an SEM image of $\alpha\text{-Fe}_2\text{O}_3$ nanoflakes on an individual microsphere. d) SEM image of $\alpha\text{-Fe}_2\text{O}_3$ nanoflakes on a glass slide. The inset picture shows the as-deposited sample (black) becomes transparent (red) after heating. e) SEM image of $\alpha\text{-Fe}_2\text{O}_3$ nanoflakes on an AFM tip. The inset is the high-magnification and side-view image of the tip. f) SEM image of $\alpha\text{-Fe}_2\text{O}_3$ nanoflakes on an electrochemically etched W tip.

nanoflakes are perpendicular to the local surface.

Glancing-angle X-ray diffraction (GAXRD, Figure 3a) and micro-Raman spectroscopy (Figure 3b) measurements show that the surface of the heated sample (Si substrate) consists of $\alpha\text{-Fe}_2\text{O}_3$ and Fe_3O_4 . Transmission electron microscopy (TEM, Figure 3c), selected area electron diffraction (SAED, Figure 3c, inset) and high resolution TEM (HRTEM, Figure 3d) further reveal that the nanoflakes are single-crystalline $\alpha\text{-Fe}_2\text{O}_3$ and free from an amorphous layer.^[17–19] A layer of condensed film, mainly

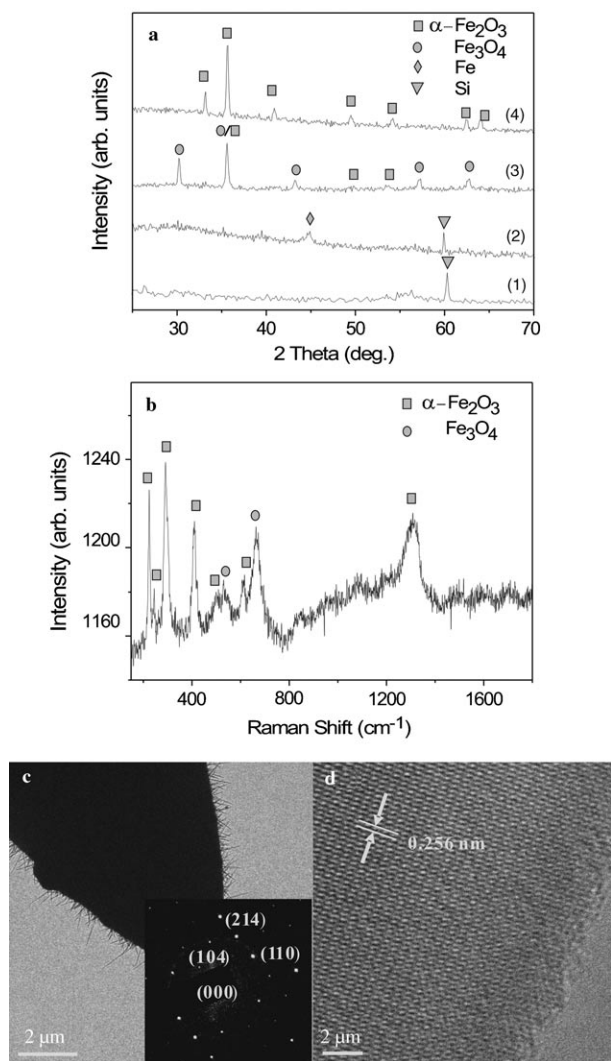


Figure 3. a) GAXRD patterns of plain Si (1), the as-deposited Fe film (2), and Fe films heated at 300 °C for 5 h and 12 h (3 and 4, respectively). b) The Raman spectrum of an Fe film heated at 300 °C for 5 min. The surface of the product consists of Fe₃O₄ and α -Fe₂O₃. c) TEM image of α -Fe₂O₃ nanoflakes on a W tip. The inset is an electron diffraction pattern of nanoflakes. d) HRTEM image of nanoflakes showing the good agreement with the diffraction pattern of α -Fe₂O₃, as shown by the zone axis of [441] and the (110) lattice spacing of $d=0.252$ nm.^[19] The nanoflakes are α -Fe₂O₃, and the condensed film is dominated by Fe₃O₄.

Fe₃O₄^[17,18] (Figure 2b), acts as the precursor for the growth of α -Fe₂O₃ nanoflakes. As the α -Fe₂O₃ nanoflakes could be directly synthesized onto different substrates with ease, a number of further investigations could be carried out to extend and improve the applications of α -Fe₂O₃. For example, the field-emission properties of α -Fe₂O₃ nanoflakes synthesized on a Si substrate, AFM tips, or W tips (as discussed below) could be studied; and optical studies of this new 2D morphology of α -Fe₂O₃ on the quartz or glass slide samples could be carried out, since these samples become transparent after heating (Figure 2d, inset).

The exact growth mechanism of α -Fe₂O₃ nanoflakes remains unclear in the present study. Considering the electron microscopy observations and the low formation temperature

(300 °C), it is unlikely that VLS or VS processes are responsible for the growth of nanoflakes. We direct air at a very high flow rate ($\approx 9 \times 10^5$ sccm) towards the sample during the growth process. This high-speed air flow ensures that not much vapor stays above the sample surface. The SEM images reveal the nanoflakes formed have similar morphologies as those fabricated without air flow. This suggests that the role of a vapor phase may not be significant during the growth process. We propose the solid–liquid–solid (SLS) mechanism for the growth of α -Fe₂O₃ nanoflakes. Basically, when the temperature of the hotplate is high enough, the surface layer of Fe foil/film or even the native Fe oxide layer starts to melt and forms a liquid medium (see Figure 4

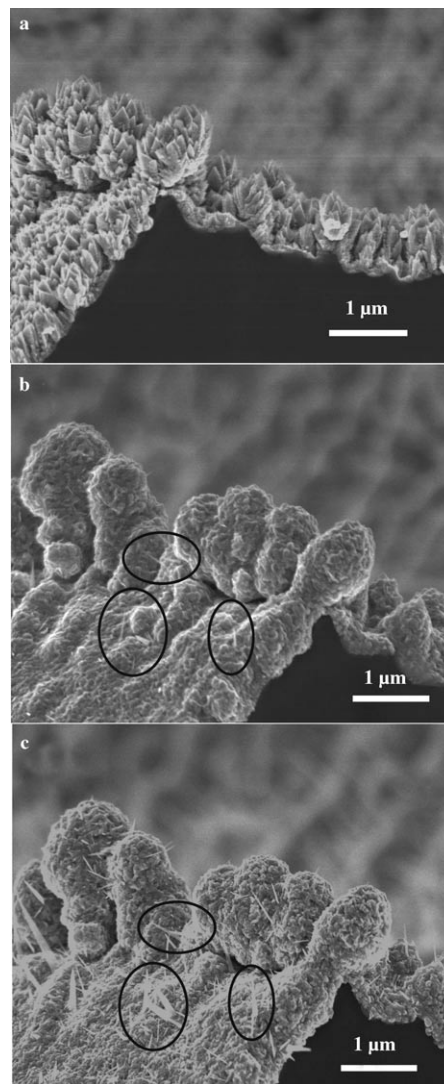


Figure 4. a) SEM image of the as-deposited Fe film on Si. b) The Fe film in (a) heated at 300 °C for 3 min; the melting of the surface layer and the rapid growth of α -Fe₂O₃ nanoflakes (highlighted in the circles) is shown. c) SEM image of the sample in (b) heated at 300 °C for 5 min; the new and continuous (same regions as indicated in b) growth of nanoflakes is shown. The α -Fe₂O₃ nanoflakes could be synthesized by directly heating an Fe film (a) or an Fe film with a thin layer of oxide (b). The density and the size of such nanoflakes could be simply controlled by varying the heating duration (see Supporting Information).

for sequential images taken at different stages of the growth process). Subsequently, this liquid medium may adsorb the oxygen in air and be oxidized to Fe_3O_4 , which acts as the precursor (or intermediate) for growth of $\alpha\text{-Fe}_2\text{O}_3$ nanoflakes. The formation of the precursor may play an important role in the low-formation-temperature process.^[1] The $\alpha\text{-Fe}_2\text{O}_3$ nanoflakes begin to grow when the Fe_3O_4 near the surface is further oxidized, and the $\alpha\text{-Fe}_2\text{O}_3$ precipitates from the liquid medium after supersaturation. The growth continues until cooling down, when the liquid is condensed into the solid state. It is noted that the as-deposited Fe film (Figure 4a) consists of regular-shaped nanoparticles, which seem to evolve in the further nanoflake growth. However, considering the successful growth of nanoflakes with the same morphology starting with Fe foil (Figure 1d), where the particles show a different morphology compared with that of the deposited Fe film, the growth of $\alpha\text{-Fe}_2\text{O}_3$ nanoflakes may not pre-require the regular-shaped Fe particles. Furthermore, the as-deposited Co and Zn particles (images shown below) do not show any particular shape, and further one-dimensional (1D) or 2D oxide nanostructures could be formed by heating the same as-deposited films. Thus, the growth of metal oxide nanostructures using our hotplate method may not strongly depend on the morphology of the initial metal particles.

In this work, we have also studied the field-emission properties of the $\alpha\text{-Fe}_2\text{O}_3$ nanoflakes using field emission microscopy (FEM). By directly synthesizing nanoflakes on the etched W tip, it is possible to investigate the field-emission properties of a small number of emitters.^[20] Figure 5a shows the field-emission current–voltage (I – V) curve. Under a voltage of 1.26 kV, an emission current of $0.8\ \mu\text{A}$ is obtained. The corresponding Fowler–Nordheim (FN)^[21] plot (Figure 5a, inset) shows a straight line when the current is larger than 1 nA, suggesting that tunneling emission occurs.^[22] By fitting the FN plot, an enhancement factor of about $6 \times 10^5\ \text{cm}^{-1}$ can be estimated.^[23] Compared with carbon nanotubes (enhancement factor of about $2.4 \times 10^5\ \text{cm}^{-1}$),^[24] such a high enhancement factor should be related to the tip-shape geometry of the W substrate and to the multiple emitters involved in the field emission. By applying an acceleration voltage,^[25] the short-term stability and FEM images at different current levels are studied (Figure 5b). It is observed that the current fluctuation increases with current level. Considering the ultrahigh vacuum in FEM, such a high level of current fluctuation can be ascribed to the shifting of emitting sites between nanoflakes,^[26] which is also consistent with the corresponding FEM image and video.^[27] It is believed that the $\alpha\text{-Fe}_2\text{O}_3$ nanoflakes may be a potential candidate for future electron-emitter devices due to their high enhancement factor and substrate-friendly synthesis.

To further extend the substrate-friendly synthesis of metal oxide nanostructures using this hotplate method, we deposited Co and Zn films on different types of substrates and heated the films at various temperatures in air. SEM images (Figure 6) reveal Co_3O_4 and ZnO nanostructures could be successfully fabricated. More excitingly, the morphologies of the Co_3O_4 and ZnO nanostructures are temperature dependent. This implies that the hotplate technique

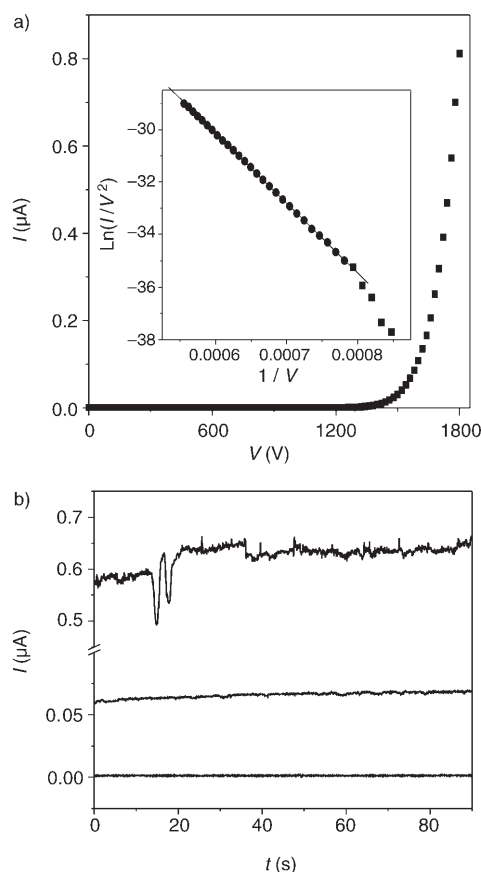


Figure 5. Field-emission properties of $\alpha\text{-Fe}_2\text{O}_3$ nanoflakes on a W tip. a) Typical field-emission current–voltage (I – V) curve from the $\alpha\text{-Fe}_2\text{O}_3$ nanoflakes on the W tip (Figure 2 f). The voltage is swept from 0 to 1800 V in steps of 20 V. Before sweeping, the emitters were conditioned by heating at about $600\ ^\circ\text{C}$ to remove residual gas adsorbates on the nanoflakes. The inset depicts the FN plot ($\ln(I/V^2)$ versus $1/V$), showing a perfect linear dependence. b) Short-term stability at different current levels.

may provide reasonable control of the morphology during synthesis of metal oxide nanostructures.

The successful synthesis of single-crystalline metal oxide nanostructures on a large scale and at low-cost by directly heating the appropriate metals at low temperatures in air demonstrates the hotplate method could be a powerful material supplier for further fundamental research and industrial applications. Moreover, this technique may provide an alternative method or open a new approach to the simple fabrication of metal oxide nanostructures at low temperatures, especially for those metals with high melting points. The simple and open system used in our approach also provides much flexibility in carrying out in situ investigations, that is, in situ XRD, in situ micro-Raman spectroscopy, to study the detailed growth mechanisms of metal oxide nanostructures.

Experimental Section

To synthesize $\alpha\text{-Fe}_2\text{O}_3$ nanoflakes, we heated polished and cleaned Fe foil (Aldrich, 0.1 mm thick, 99.9+ %) on a hotplate

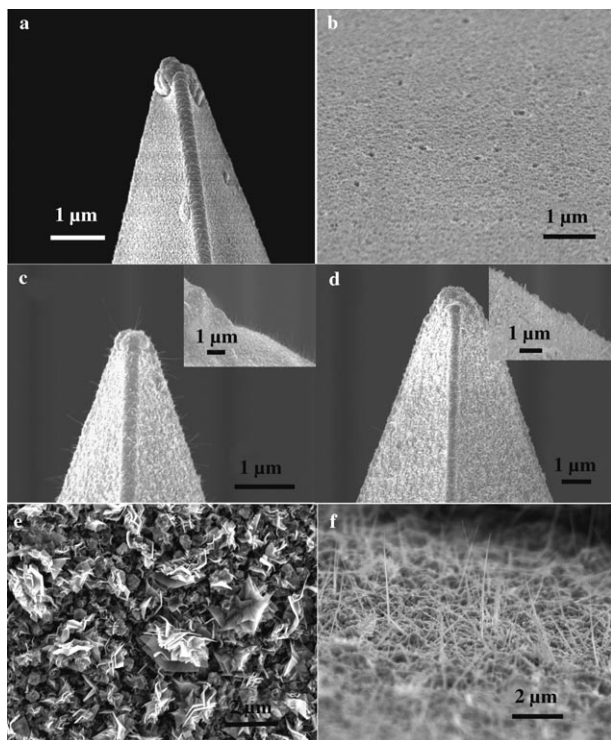


Figure 6. SEM images of metal oxide nanostructures on different types of substrates. a,b) SEM images of as-deposited Co and Zn on an AFM tip and Si, respectively. c,d) SEM images of Co_3O_4 nanostructures synthesized by heating Co film on AFM tips at 250 °C and 450 °C, respectively, for 30 min. The insets are SEM images of the lower parts of the tips. The dominant morphologies seem to be controlled as wirelike (c) or flakelike (d) by varying the heating temperatures. e,f) SEM images of ZnO nanostructures fabricated by heating Zn film on a Si wafer at 275 °C for 30 min or 375 °C for 12 h, respectively, showing that 2D or 1D nanostructures (e and f, respectively) could be selectively formed at different heating temperatures.

at 300 °C for various durations (10 min to 24 h) in air. For the development of a new, substrate-friendly synthesis of metal oxide nanostructures, the appropriate metal films were first deposited directly onto the substrates by radio-frequency magnetron sputtering (Denton vacuum Discovery18 system), and the coated substrates were subsequently heated on a hotplate in air. Typical film thickness ranges from 300 to 900 nm. The Fe foil, as-deposited metal films, and surface layer of heated products were characterized and analyzed by SEM (JEOL JSM-6400F), GAXRD (Bruker Analytical X-Ray System, $\text{CuK}\alpha$ radiation, $\lambda = 1.5406 \text{ \AA}$), micro-Raman spectroscopy (ISA T640000 Triple Grating System, Ar laser, $\lambda = 514.5 \text{ nm}$), and TEM (JEOL JEM-2010F, 200 kV).

Keywords:

metal oxides • nanostructures • self-assembly • synthesis design

[1] Y. Xia, P. Yang, Y. Sun, Y. Wu, B. Mayers, B. Gates, Y. Yin, F. Kim, H. Yan, *Adv. Mater.* **2003**, *15*, 353–389.

[2] a) A. Kolmakov, M. Moskovits, *Annu. Rev. Mater. Res.* **2004**, *34*, 151–180; b) C. Lee, T. Lee, S. Lyu, Y. Zhang, H. Ruh, H. Lee, *Appl. Phys. Lett.* **2002**, *81*, 3648–3650; c) P. Poizot, S. Laruelle, S. Grugeon, L. Dupont, J.-M. Tarascon, *Nature* **2000**, *407*, 496–499; d) M. Huang, S. Mao, H. Feick, H. Yan, Y. Wu, H. Kind, E. Weber, R. Russo, P. Yang, *Science* **2001**, *292*, 1897–1899; e) H. Kind, H. Yan, M. Law, B. Messer, P. Yang, *Adv. Mater.* **2002**, *14*, 158–160.

[3] X. Jiang, Y. Wang, T. Herricks, X. Xia, *J. Mater. Chem.* **2004**, *14*, 695–703.

[4] P. Yang, C. Lieber, *Science* **1996**, *273*, 1836–1840.

[5] M. Huang, Y. Wu, H. Feick, E. Webber, P. Yang, *Adv. Mater.* **2000**, *12*, 113–116.

[6] Y. Zhang, N. Wang, S. Gao, R. He, S. Miao, J. Liu, J. Zhu, X. Zhang, *Chem. Mater.* **2002**, *14*, 3564–3568.

[7] H. Dang, J. Wang, S. Fan, *Nanotechnology* **2003**, *14*, 738–741.

[8] P. Zheng, Z. Dai, Z. Wang, *Science* **2001**, *291*, 1947–1949.

[9] L. Greene, M. Law, J. Goldberger, F. Kim, J. Johnson, Y. Zhang, R. Saykally, P. Yang, *Angew. Chem.* **2003**, *115*, 3139–3142; *Angew. Chem. Int. Ed.* **2003**, *42*, 3031–3034.

[10] T. Yu, X. Zhao, Z. Shen, Y. Wu, W. Su, *J. Cryst. Growth* **2004**, *268*, 590–595.

[11] The ZnO nanostructures were fabricated by directly heating the Zn foil in air at 350 °C using a hotplate.

[12] T. Yu, Y. Zhu, X. Xu, Z. Shen, P. Chen, C.-T. Lim, J. Thong, C.-H. Sow, *Adv. Mater.* **2005**, *17*, 1595–1599.

[13] <http://www.webelements.com/webelements/elements/text/Fe/heat.htm1>

[14] a) J. Chen, L. Xu, W. Li, X. Gou, *Adv. Mater.* **2005**, *17*, 582–586; b) M. Gondal, A. Hameed, Z. Yamani, A. Suwaiyan, *Chem. Phys. Lett.* **2004**, *385*, 111–115; c) H. Kung, *Transition Metal Oxides: Surface Chemistry and Catalysis*, Elsevier, New York, **1989**.

[15] J. Ji, S. Ohkoshi, K. Hashimoto, *Adv. Mater.* **2004**, *16*, 48–51.

[16] K. Woo, H. Lee, J. Ahn, K. Park, *Adv. Mater.* **2003**, *15*, 1761–1764.

[17] S. Lian, E. Wang, Z. Kang, Y. Bai, L. Gao, M. Jiang, C. Hu, L. Xu, *Solid State Commun.* **2004**, *129*, 485–490.

[18] D. de Faria, S. Silva, M. de Oliveira, *J. Raman Spectrosc.* **1997**, *28*, 873–878.

[19] Joint Committee on Powder Diffraction Standards (JCPDS), Card No. 33-0664, hematite ($\alpha\text{-Fe}_2\text{O}_3$).

[20] J. Zhang, J. Tang, G. Yang, Q. Qiu, L.-C. Qin, O. Zhou, *Adv. Mater.* **2004**, *16*, 1219–1222.

[21] R. Fowler, L. W. Nordheim, *Proc. R. Soc. London Ser. A* **1928**, *119*, 173–181.

[22] J. W. Gadzuk, E. W. Plummer, *Rev. Mod. Phys.* **1973**, *45*, 487–548.

[23] Here the enhancement factor (β) is defined as $F = \beta V$, where F is the local electric field in the FN equation (ref. [27]), and V is the applied voltage in our measurements. From the FN equation, the slope (S) of the FN plot depends on the enhancement factor by $S = B/\beta$, where B is a constant with an approximate value of $6.44 \times 10^7 \text{ Vcm}^{-1} \text{ eV}^{-3/2}$.

[24] D. Lovall, M. Buss, E. Graugnard, R. P. Andres, R. Reifenberger, *Phys. Rev. B* **2000**, *61*, 5683–5691.

[25] The acceleration voltage is defined here as the voltage between the anode ring and the screen with phosphor coating to produce enough brightness. In our FEM experiments, the acceleration voltage was 3.2 kV. It is worth noting that this voltage will penetrate the region between anode and cathode and affect the actual field on the surface of emitters.

[26] P. G. Collins, A. Zettl, *Phys. Rev. B* **1997**, *55*, 9391–9399.

[27] Supporting information data contains FEM images and a table showing the dependence of density and size on the heating duration.

Received: July 13, 2005

Published online on October 20, 2005